Applied Thermal Engineering 242 (2024) 122411

Contents lists available at ScienceDirect

Applied Thermal Engineering

journal homepage: www.elsevier.com/locate/apthermeng

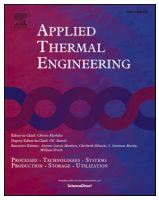

Research Paper

Efficient hydraulic and thermal simulation model of the multi-phase natural gas production system with variable speed compressors

Wendi Xue [a], Yi Wang [a,*], Yuejiu Liang [b], Tianfu Wang [a], Bowen Ren [c]

[a] National Engineering Research Center of Oil and Gas Pipeline Transportation Safety/MOE Key Laboratory of Petroleum Engineering/Beijing Key Laboratory of Urban Oil and Gas Distribution Technology, China University of Petroleum (Beijing), Beijing 102249, China
[b] PetroChina Planning & Engineering Institute, No.3 Zhixin West Road, Haidian District, Beijing 100089, China
[c] Tian Hua Institute of Chemical Machinery and Automation, No. 3 North Heshui Road, Xigu District, Lanzhou 730030, China

ARTICLE INFO

Keywords:
Pipe network
Numerical simulation
Natural gas
Multi-phase flow
Compressor model

ABSTRACT

The natural gas production system is a very complex system, involving pipelines, compressors and valves with different structures and calculation parameters. It can be divided into two different parts: gas production and collection pipe networks. Fluid flow in the gas production pipe network is multi-phase flow. Fluid flow in the gas collection pipe network is single-phase flow. It is imperative to consider gas production and collection pipe networks in conjunction to ensure accurate operation simulation. The complexity of the network structures and flow statuses can cause computational instability or even divergence problems in simulations when coupling these two types of pipe networks. To address this issue, an automatic and practical node numbering method is proposed for the large-scale pipe network, which can ensure the full rank of the solution matrix and computational stability. On the other hand, due to the need for frequent adjustments of the pipe networks to satisfy the production demand, computational boundary treatments of constant inlet/outlet pressure, constant flow rate or constant pressure ratio for the compressor stations are not suitable. To address this issue, the characteristic curves of compressors are coupled into the simulation of pipe networks to represent the variable-speed centrifugal and reciprocating compressors.

The accuracy and robustness of the proposed models and numerical methods are validated through comparisons with software results and field data. The simulation time is only within 0.5 s for the natural gas production system with 210 nodes and 176 pipelines. Our model has relative deviations within 3% in both pressure and flow rate compared to field data and within 10% compared to software.

1. Introduction

Natural gas is a clean, efficient, and renewable energy source, whose development and utilization has significant economic and environmental implications. However, natural gas production system is highly large and complex. It contains production pipe networks connecting production wells to collection stations, and collection pipe networks connecting collection stations to the purification plant [1–3]. These networks can contain several hundreds of pipelines with complex topological connections [4–6]. As shown in Fig. 1, produced gas from wells contains water, sulfur and other impurities, so the fluid flow in the production pipe network is typically multi-phase. Moreover, initial purified gas in the collection station is natural gas without impurities, so the fluid flow in the collection pipe network is typically single-phase.

With the development of exploitation, the scale of the natural gas production system becomes larger and more complex while the production rates of wells decrease [7–9]. These variations require the adjustment of the operating parameters of the system via compressors accurately in time. Artificial operations by workers' hands cannot satisfy the requirement of real-time adjustment. Therefore, the automatic control is needed. Robust and efficient numerical simulation is the core of the automatic control. Based on the complexity of this natural gas production system, we will illustrate major improvements of this study in the following three parts:

(1) Topology modelling of pipe network with complex structure.
(2) Efficient hydraulic and thermal numerical method for the complex network coexisting single-phase flow and multi-phase flow.

* Corresponding author.
E-mail addresses: xuewendi@126.com (W. Xue), wangyi1031@cup.edu.cn (Y. Wang).

https://doi.org/10.1016/j.applthermaleng.2024.122411
Received 22 September 2023; Received in revised form 8 December 2023; Accepted 8 January 2024
Available online 12 January 2024

Nomenclature

m	number of nodes
n	number of pipelines
$\boldsymbol{A} = [a_{ij}]_{m\times n}$	incidence matrix of network structure
$\boldsymbol{Y}$	incidence matrix of node gas pressure and flow rate ($Pa^{-1}\cdot m^3\cdot s^{-1}$)
P	square of gas pressure (Pa^2)
$\boldsymbol{P}$	vector of square of gas pressure (Pa^2)
ΔP	square difference of gas pressure (Pa^2)
$\Delta \boldsymbol{P}$	vector of square difference of gas pressure (Pa^2)
q	gas volume flow rate ($m^3\cdot s^{-1}$)
$\boldsymbol{q}$	vector of gas volume flow rate ($m^3\cdot s^{-1}$)
Q	gas volume flow rate at standard conditions ($m^3\cdot s^{-1}$)
$\boldsymbol{Q}$	vector of gas volume flow rate at standard conditions ($m^3\cdot s^{-1}$)
C	coefficient related to unit of the pressure drop model ($Pa^{-1}\cdot m\cdot s^{-1}\cdot K^{0.5}$)
p	gas pressure (Pa)
d	inner diameter (m)
λ	friction factor
Z	gas compression factor
Δ	gas relative density
T	gas temperature (K)
L	pipeline length (m)
α	index related to the friction factor equation
SS	coefficient related to the gas volume flow rate ($Pa^2\cdot m^{-3\alpha}\cdot s^{\alpha}$)
T_0	environmental temperature (K)
a_T	coefficient related to heat transfer (m^{-1})
D_i	gas Joule-Thomson coefficient ($Pa^{-1}\cdot K$)
M	gas mass flow rate ($kg\cdot s^{-1}$)
u	flow velocity ($m\cdot s^{-1}$)
u_{sg}	gas apparent flow velocity ($m\cdot s^{-1}$)
H	cross-sectional content
ρ_l	density ($kg\cdot m^{-3}$)
x	gas mass fraction
c_p	specific heat capacity ($J\cdot kg^{-1}\cdot K^{-1}$)
b_0	coefficient related to the friction (K)
a, b, c	parameters of the equipment model
d	parameter of the equipment model, units are not unique (Pa^2 or $m^3\cdot s^{-1}$)
H	compressor available energy head (m)
m	gas variability index
R_g	gas constant ($J\cdot kg^{-1}\cdot K^{-1}$)
n	compressor rotational speed (rpm)
n_0	compressor reference rotational speed (rpm)
a_1	coefficient of the centrifugal compressor (m)
b_1	coefficient of the centrifugal compressor ($m^{-2}\cdot s$)
c_1	coefficient of the centrifugal compressor ($m^{-5}\cdot s^2$)
V_h	inspiratory volume of the reciprocating compressor (m^3)
$\lambda_l, \lambda_p, \lambda_T$	coefficients of the reciprocating compressor, related to losses of gas mass, gas pressure and gas temperature, respectively
α	relative clearance volume of the reciprocating compressor
C_d	resistance coefficient of the valve

Subscripts

in	pipeline inlet
out	pipeline outlet
l	liquid for two-phase flow model
g	gas for two-phase flow model
S	standard condition

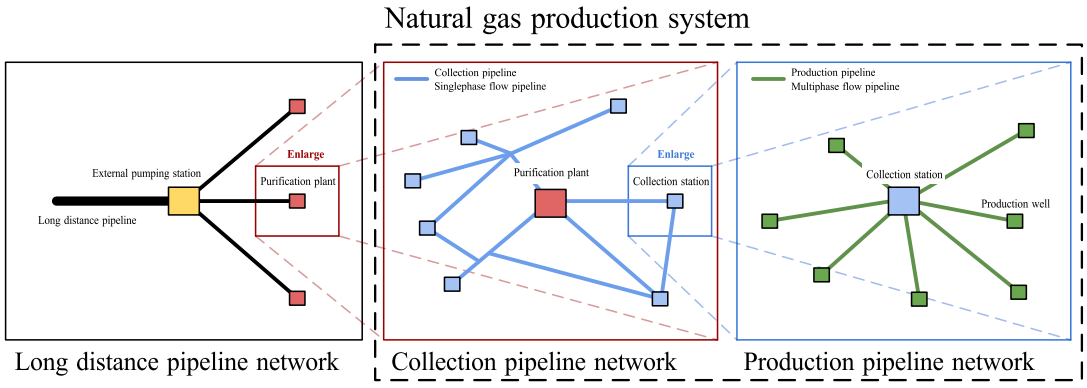

Fig. 1. Natural gas production system.

(3) Combining the operational adjustment of compressor stations with fluid flow in the network simulation.

Related works in these three parts are summarized as follows:

1.1. Topology modeling for pipe network

The topology of pipe network in the gas field has different structures, e.g. ring, branch, ring-branch etc., for different purposes. Numerical description of these complex structures is the first essential step for the numerical simulation of the whole system. Cross et al. [10] was the first to propose a method for solving ring pipe networks. Brkić et al. [11] improved the Cross model by promoting computational speed. Stoner et al. [12,13] proposed a node equation method for the simulation of pipe networks. Berard et al. [14] proposed an optimal node-numbering scheme to eliminate pivoting of the coefficient matrix and to reduce matrix "fill-in". Liu et al. [15] proposed a specific numbering approach which used to model the topology of the different networks and their linkages through conversion components. Osiadacz et al. [16–18] developed a pipe network model for arbitrary structures and analyzed the advantages and disadvantages of both the ring equation and node equation methods. Szoplik et al. [19] introduced a mathematical model

of the pipe network based on Kirchhoff's first and second laws. Taherinejad et al. [20] proposed a new approach based on an electrical analogy which leads to an algebraic and a first-order ordinary differential equation.

Most existing studies use directed graphs to model the topology of pipe networks, where equipment are nodes and pipelines are edges. Berard et al. [14] firstly considered the effect of node numbering on the computational stability of the simulation of pipe networks and proposed an available numbering method. Liu et al. [15] proposed a node numbering method for different networks. However, this numbering method is a manual method for the network, which requires manual numbering and is not applicable to complex pipe networks. Therefore, Berard's method is still the commonly used numbering method. When the two types of pipe networks are coupled, the coupling nodes are connected to compressors, which can cause divergence. The reason is that the boundary conditions of the coupling nodes and the compressor are inconsistent, which can lead solution matrix not full of rank. It leads to the failure of Berard's method. Therefore, Berard's method is not applicable to the natural gas production system that involves both single-phase and multi-phase flow pipe networks. A more efficient and automatic topological modeling method is required for this complex production system.

1.2. Numerical method for pipe network

Solvable sets of equations are obtained by topological modeling. Further, numerical method for pipe networks is crucial. It influences the computational efficiency and convergence of the solution. Cross et al. [10] also proposed a method based on head balance to correct the flow rate of the pipeline. Similarly, Szoplik et al. [19] solved the network model by correcting ring flow. Further, Martin and Peters et al. [21] applied the Newton-Raphson method to solve pipe network models. Similarly, Stoner et al. [12,13] introduced the node equation into this method. In contrast, Wood and Charles et al. [22] linearized the pipeline pressure drop equation to form a linear system of equations, thereby addressing the issue of initial values required by the Newton-Raphson method. Sun et al. [23] linearized the flow rate to establish a linear relationship between pressure drop and flow rate, eliminating the need for the calculation of the Jacobian matrix. Berard et al. [14] introduced the concept of block matrix and used LU decomposition to solve the pipe network model. López-Benito et al. [24] presented a steady-state non-isothermal flow model and suggested that the accuracy of the model is dependent on the precision of field data. Wang et al. [25] developed a fast prediction method for steady-state heat convection. Sun et al. [23] linearized the flow rate to establish a linear relationship between pressure drop and flow rate, eliminating the need for initial values or calculation of the Jacobian matrix.

The traditional methods for simulating pipe networks are based on single-phase flow, which is suitable for gas transmission pipelines that carry dry and pure natural gas. However, these methods are not applicable to the natural gas production system which has both single-phase and multi-phase flows in pipe networks. The production pipe network uses the mass flow rate as the calculation parameter, while the collection pipe network uses the volume flow rate as the calculation parameter. Therefore, two systems of equations need to be solved simultaneously, which makes the boundary setting and coupling method challenging. A more general numerical method is required to handle the complex pipe network with different calculation parameters.

1.3. Numerical treatment of compressor stations in pipe network

The compressor station is essential for the pipe network. It changes its speed to adjust flow rate in pipe network based on the production schedule. Therefore, it is important to simulate the flow and pressure changes at the compressor station accurately, affecting the accurate simulation of the pipe network. Woldeyohannes et al. [26] proposed a method for coupling the compressor and pipe network models, resulting in improved accuracy and convergence. Bermúdez et al. [27] developed a mathematical model for pipelines, compressors, and valves that couples the pipeline and equipment to form a nonlinear system of equations based on mass conservation at pipe network nodes. Pambour et al. [28] presented a linearization method to correlate pressure and flow linearly at the compressor station. Zhou et al. [29] introduced the compressor mechanism model, which simplifies the compressor as a function of pressure ratio and speed by the mapping relationship of compressor characteristics.

Previous studies assume that the compressor stations have constant inlet/outlet pressure, constant flow rate or constant pressure ratio. However, these boundary conditions are too ideal and cannot match the practical operations with variable parameters of the compressors. This limits the existing methods to simulate only the conditions with constant parameters, which are typical for transmission pipelines. Moreover, the compressor station is usually located at the outlet of the collection station and needs to be coupled with the production pipeline system. The previous boundary treatment of compressor stations simplified compressor station characteristics may lead to computational instability. Therefore, due to the need for frequent adjustments of the pipe networks to satisfy the production demand and to make the simulation suitable for variable parameters, the simulation model should include the characteristic curves and the appropriate solving methods of the compressor stations.

1.4. Major improvements of this study

This study aims to develop a set of efficient and robust methods for natural gas production system, which is a very complex system that involves both multi-phase and single-phase flows in pipe networks and compressor stations. Base on the above literature reviews and analyzes, the existing models and numerical methods are not suitable to the natural gas production system. Therefore, this study makes three improvements over the existing studies, as follows:

(1) An efficient and automatic topological modeling method that can automatically number the nodes of the network is proposed. This method resolves the boundary condition conflicts between the coupling nodes and compressor stations, which is issue that Berard's method [14] cannot handle.
(2) An efficient hydraulic and thermal simulation method that can simulate the natural gas production system is proposed. This method solves two systems of equations simultaneously, one for the production pipe network that uses the mass flow rate as the calculation parameter, and the other for the collection pipe network that uses the volume flow rate as the calculation parameter. A coupling method between the pipe networks is also proposed.
(3) Due to the need for frequent adjustments of the pipe networks to satisfy the production demand, a comprehensive compressor model that can incorporate the characteristic curves of centrifugal and reciprocating compressors and eliminate the unrealistic assumptions of constant inlet/outlet pressure, constant flow rate or constant pressure ratio. The linearized models of the compressor stations are derived, which can maintain the computational stability.

2. Robust topological modeling method

Robust topological modeling is the first key to efficient simulation of complex pipe networks. It should mathematically describe the physical structure of the pipe network to provide a basis for numerical simulation. Also, this mathematical description should be automatic instead of manual to fit any topology of different pipe networks.

Thus, in this section, a detailed overview of the structure and

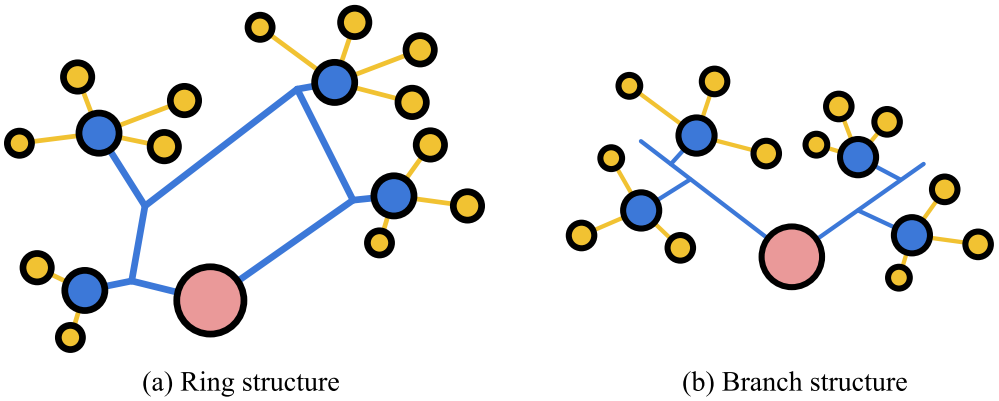

Fig. 2. Typical structures of the pipe network.

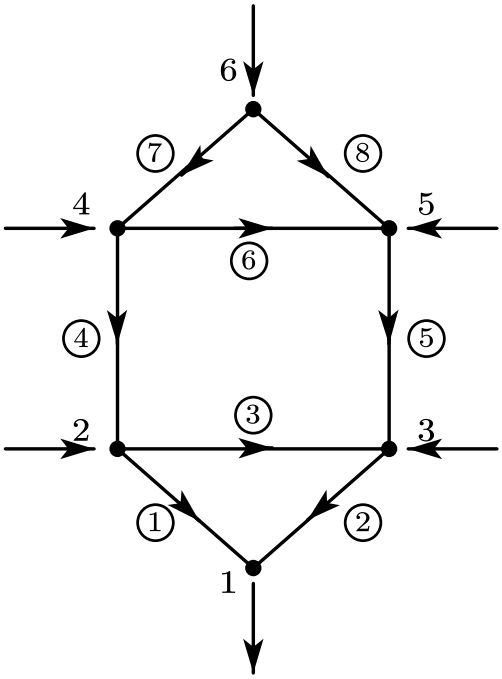

Fig. 3. Example of a pipe network.

Table 1
Inlet and outlet nodes of pipelines.

Pipeline number	Inlet node number	Outlet node number
1	2	1
2	3	1
3	2	3
4	4	2
5	5	3
6	4	5
7	6	4
8	6	5

mathematical descriptions of the natural gas production system is presented, including gas collection and production pipe networks. We analyze the factors influencing the computational stability. A new automatic node numbering method is proposed.

2.1. Structure and mathematical descriptions of pipe network

As shown in Fig. 2, the gas collection and production pipe networks are both included in the natural gas production system [30]: the gas collection pipeline system is represented in the blue area, the yellow area is for the gas production pipeline system, and the pink is for the purification plant, which is the terminal node:

(1) Multi-phase gas is transported from wellheads to collection stations in the gas production pipeline. Several wellheads are connected to a single collection station. Its network structure is relatively simple.
(2) Single-phase gas preliminarily separated at the collection station is transported to the purification plant in the gas collection pipeline. The gas collection pipe network can be divided into the structures of ring and branch. Its network structure is highly complex and includes both structures, which are difficult to distinguish.

As shown in Fig. 3, the pipe network can be represented as a directed graph composed of nodes and edges. Nodes are represented as wellheads, collection stations, purification plants, and connection points. These nodes are interconnected by edges which are defined as pipelines. The direction of the edge indicates the positive flow direction within the corresponding pipeline.

The network shown in Fig. 3 includes six nodes and eight pipelines. Node 1 is the flow outflow boundary, while nodes 2, 3, 4, and 5 are the flow inflow boundaries. The inlet and outlet nodes of each pipeline are presented in Table 1.

Table 1 can be represented in matrix form as an incidence matrix (Eq. (1)) [17]. Given a pipe network with n pipelines and m nodes, the incidence matrix $\boldsymbol{A} = [a_{ij}]_{m\times n}$ of order $m \times n$ can be constructed: 1 indicates that the outlet node of pipeline j is node i; -1 indicates that the inlet node of pipeline j is node i; 0 indicates that node i is not connected to pipeline j, as follows:

$$\boldsymbol{A} = \begin{bmatrix} 1 & 1 & 0 & 0 & 0 & 0 & 0 & 0 \\ -1 & 0 & -1 & 1 & 0 & 0 & 0 & 0 \\ 0 & -1 & 1 & 0 & 0 & 0 & 0 & 0 \\ 0 & 0 & 0 & -1 & 0 & -1 & 1 & 0 \\ 0 & 0 & 0 & 0 & -1 & 1 & 0 & 1 \\ 0 & 0 & 0 & 0 & 0 & 0 & -1 & -1 \end{bmatrix} \tag{1}$$

The incidence matrix $\boldsymbol{A}$ effectively captures the connectivity of the pipe network between nodes and edges.

2.2. Effect of node numbering method

During the solving process, it is observed that node numbering significantly impacts computational stability. This necessitates frequent

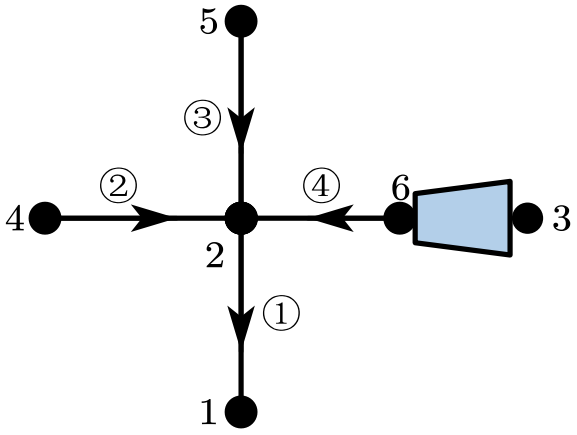

Fig. 4. Initial node numbering of case 1.

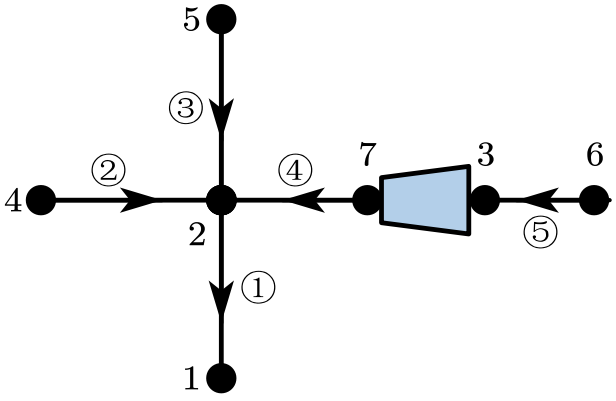

Fig. 5. Updated node numbering of case 1.

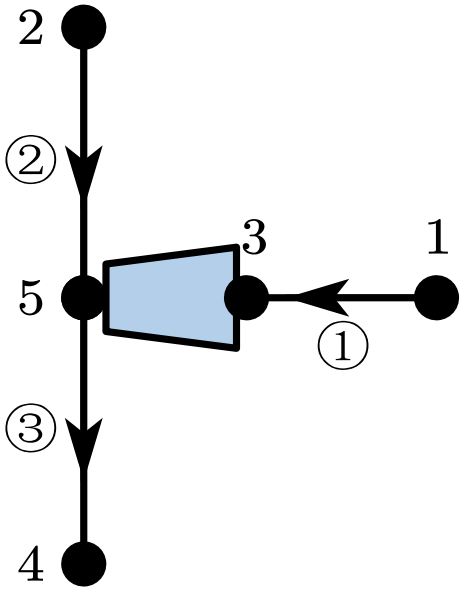

Fig. 6. Initial node numbering of case 2.

manual adjustments to node numbers. A node numbering method that ensures stability is proposed to address this problem. Taking the linear approximation method as an example, the system of equations can be obtained as follows:

$$-\boldsymbol{YP} = \boldsymbol{q} \tag{2}$$

where $\boldsymbol{Y}$ is the incidence matrix of node pressure and flow rate, which is derived in section 4.2 and has the boundary condition specified in section 4.1. $\boldsymbol{P} = [P_1, P_2, \cdots, P_m]^{\mathrm{T}}$ is the vector of node pressure, $\boldsymbol{q} = [q_1, q_2, \cdots, q_n]^{\mathrm{T}}$ is the vector of node flow rate. A block iteration method [10] is adopted to calculate the nodes with different boundary conditions as follows:

$$\begin{bmatrix} \boldsymbol{Y}_{11} & \boldsymbol{Y}_{12} \\ \boldsymbol{Y}_{21} & \boldsymbol{Y}_{22} \end{bmatrix} \begin{bmatrix} \boldsymbol{P}_1 \\ \boldsymbol{P}_2 \end{bmatrix} = \begin{bmatrix} -\boldsymbol{q}_1 \\ -\boldsymbol{q}_2 \end{bmatrix} \tag{3}$$

In the Eq. (3), $\boldsymbol{P}_1$ and $\boldsymbol{q}_2$ are the unknown node pressure and flow rate, respectively. $\boldsymbol{P}_2$ and $\boldsymbol{q}_1$ are the known node pressure and flow rate, respectively, i.e. the boundary nodes. The system of equations is iterated into two steps: (1) According to $\boldsymbol{Y}_{11}$ and $\boldsymbol{Y}_{12}$, $\boldsymbol{P}_1$ is solved; (2) According to $\boldsymbol{Y}_{21}$ and $\boldsymbol{Y}_{22}$, $\boldsymbol{q}_2$ is updated. In the following, we discuss the stability of the matrix $\boldsymbol{Y}$ through cases.

2.2.1. Case 1

2.2.1.1. Overlapping nodes. As shown in Fig. 4, node 1 is the flow boundary node. Nodes 3, 4, and 5 are the pressure boundary nodes. Nodes 3 and 6 are the inlet and outlet nodes for the equipment, respectively.

The matrix $\boldsymbol{Y}$ (Eq. (4)) is obtained using the above node numbering as follows:

$$\mathbf{Y} = \left[\begin{array}{ccc:ccc} y_1 & -y_1 & 0 & 0 & 0 & 0 \\ -y_1 & y_1+y_2+y_3+y_4 & 0 & -y_2 & -y_3 & -y_4 \\ 0 & 0 & 0 & 0 & 0 & 0 \\ \hdashline 0 & -y_2 & 0 & y_2 & 0 & 0 \\ 0 & -y_3 & 0 & 0 & y_3 & 0 \\ 0 & -y_4 & 0 & 0 & 0 & y_4 \end{array}\right] \tag{4}$$

Due to the lack of connection between node 3 and the pipeline, the matrix is not full rank and cannot be iterated appropriately. Thus, overlapping nodes may result in an unranked matrix and negatively impact computational stability. As shown in Fig. 5, an auxiliary pipeline is introduced between nodes 3 and 6 to enhance stability.

The new matrix $\boldsymbol{Y}$ (Eq. (5)) is obtained using the above node numbering as follows:

$$\mathbf{Y} = \left[\begin{array}{ccc:cccc} y_1 & -y_1 & 0 & 0 & 0 & 0 & 0 \\ -y_1 & y_1+y_2+y_3+y_4 & 0 & -y_2 & -y_3 & 0 & -y_4 \\ 0 & 0 & y_5 & 0 & 0 & -y_5 & 0 \\ \hdashline 0 & -y_2 & 0 & y_2 & 0 & 0 & 0 \\ 0 & -y_3 & 0 & 0 & y_3 & 0 & 0 \\ 0 & 0 & -y_5 & 0 & 0 & y_5 & 0 \\ 0 & -y_4 & 0 & 0 & 0 & 0 & y_4 \end{array}\right] \tag{5}$$

Due to the addition of auxiliary pipelines, the matrix $\boldsymbol{Y}_{11}$ is full rank. This approach can also be applied to other cases of overlapping nodes, such as flow boundary nodes overlapping with equipment nodes or equipment nodes overlapping with other equipment nodes.

2.2.2. Case 2

2.2.2.1. Equipment inlet and outlet nodes. As shown in Fig. 6, nodes 1 and 2 are the flow boundary node. Node 4 is the pressure boundary nodes. Nodes 3 and 5 are the inlet and outlet nodes for the equipment, respectively.

The matrix $\boldsymbol{Y}$ (Eq. (6)) is obtained using the above node numbering as

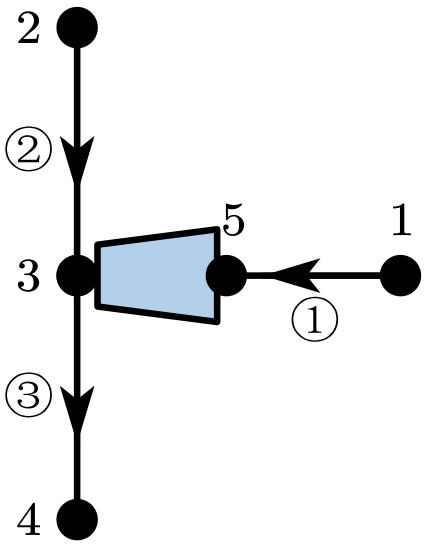

Fig. 7. Updated node numbering of case 2.

follows:

$$\mathbf{Y}=\left[\begin{array}{ccc:cc} y_1 & 0 & -y_1 & 0 & 0 \\ 0 & y_2 & 0 & 0 & -y_2 \\ -y_1 & 0 & y_1 & 0 & 0 \\ \hdashline 0 & 0 & 0 & y_3 & -y_3 \\ 0 & -y_2 & 0 & -y_3 & y_2+y_3 \end{array}\right] \tag{6}$$

Due nodes 1 and 3 are both flow boundaries. the pipeline ① lacks a pressure reference, resulting in the matrix $\boldsymbol{Y}$ not being full rank. In this case, the inlet node of equipment cannot be set as the flow boundary. As shown in Fig. 7, the inlet and outlet boundary conditions of equipment are switched, and a new node numbering is obtained.

The new matrix $\boldsymbol{Y}$ (Eq. (7)) is obtained using the above node numbering as follows:

$$\mathbf{Y}=\left[\begin{array}{ccc:cc} y_1 & 0 & 0 & 0 & -y_1 \\ 0 & y_2 & -y_2 & 0 & 0 \\ 0 & -y_2 & y_2+y_3 & 0 & -y_3 \\ \hdashline 0 & 0 & -y_3 & y_3 & 0 \\ -y_1 & 0 & 0 & 0 & y_1 \end{array}\right] \tag{7}$$

It is determined that the matrix $\boldsymbol{Y}_{11}$ is full rank. However, this node numbering method is not general. The boundary conditions of the inlet and outlet of the equipment cannot be changed manually. But this case is similar to Case 1, the method of adding an auxiliary pipeline still works.

2.2.3. Proposed node numbering method

Based on the analysis of Cases 1 and 2, a general node numbering rule is proposed to improve the automation of hydraulic and thermal simulations of gas field pipe networks. The proposed node numbering rules are shown as follows:

The dotted lines are the auxiliary pipelines. The nodes are numbered sequentially according to Fig. 8.

3. Simulation method combining single-phase and multi-phase flows in pipe network

3.1. Hydraulic and thermal models of pipelines and nodes

In contrast to long-distance pipelines, gas field pipelines are characterized by shorter lengths and more minor variations in elevation. The flow media within the collection pipeline is single-phase natural gas. Thus, the pressure drop model for horizontal gas [31,32] is adopted as the hydraulic model as follows:

$$Q=C\sqrt{\frac{\left(p_{in}^2-p_{out}^2\right)d^5}{\lambda Z\Delta TL}} \tag{8}$$

where Q is the gas volume flow rate at standard conditions, C is the coefficient related to units of the pressure drop model, p_{in} and p_{out} are the gas pressure at the inlet and outlet nodes of the pipeline, respectively, d is the pipeline inner diameter, λ is the friction factor, Z is the gas compression factor, Δ is the gas relative density, T is the gas temperature, L is the pipeline length. A relationship between pressure drop and volume flow rate can be described in Eq. (8), which can also be expressed in Eq. (9), as follows:

$$\Delta P=SQ^{\alpha} \tag{9}$$

where $\Delta P=p_{in}^2-p_{out}^2$ is the square difference of gas pressure. In this study, all P indicates p^2, S is the coefficient related to the gas volume flow rate, α is the index related to the friction factor equation.

Further, the Sukhov model for gas pipelines [31,32] is adopted as the thermal model as follows:

$$T=T_0+(T_{in}-T_0)\frac{1-e^{-a_TL}}{a_TL}-D_i\frac{p_{in}-p_{out}}{a_TL}\left[1-\frac{1-e^{-a_TL}}{a_TL}\right] \tag{10}$$

where T_0 is the environmental temperature, T_{in} is the gas temperature at the inlet node of the pipeline, a_T is the coefficient related to heat transfer, D_i is the gas Joule-Thomson coefficient.

The flow media in the gas production pipeline is the multi-phase produced gas which may contain some water [33]. The Beggs-Brill pressure drop model [34] for horizontal pipelines with low liquid holding rate flows is adopted as the hydraulic model as follows:

$$p_{in}-p_{out}=\frac{\lambda L\frac{2uM}{\pi d^3}}{1-uu_{sg}\frac{H_l\rho_l+H_g\rho_g}{p}} \tag{11}$$

where u is the flow velocity, u_{sg} is the gas apparent flow velocity, H_l and H_g are the liquid and gas cross-sectional content, respectively, ρ_l and ρ_g are the liquid and gas density, respectively. The Beggs-Brill pressure drop model is an empirical formulation with numerous relevant parameters, detailed in Beggs and Brill's study [34].

The thermal model for the collection pipelines differs slightly from the model for the production pipelines as the influence of liquid must be considered. Thus, the thermal model is adopted as the Sukhov model [35] for two-phase flow as follows:

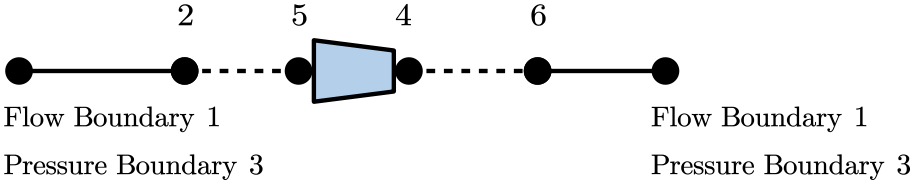

Fig. 8. General node numbering rule.

Table 2
General model parameters.

Model parameters	a	b	c	d
Constant inlet pressure	1	0	0	P_{set}
Constant outlet pressure	0	1	0	P_{set}
Constant flow rate	0	0	1	Q_{set}
Constant pressure ratio r	$\sqrt{r}$	1	0	0

$$T = (T_0 + b_0) + (T_{in} - T_0 - b_0)\frac{1 - e^{-a_T L}}{a_T L} - D_i \frac{x c_{pg}}{c_p}\frac{p_{in} - p_{out}}{a_T L}\left[1 - \frac{1 - e^{-a_T L}}{a_T L}\right] \tag{12}$$

where x is the gas mass fraction, c_{pg} is the gas specific heat capacity, c_p is the average specific heat capacity of the two phases, b_0 is the coefficient related to the friction.

Furthermore, the equal fluxes at the inlet and outlet of pipelines should be satisfied for the nodes. This can be expressed mathematically as follows:

$$\sum_{i\in in}|Q_i| = \sum_{i\in out}|Q_i| \text{ or } \sum_{i\in in}|M_i| = \sum_{i\in out}|M_i| \tag{13}$$

$$\underset{i\in in, j\in out}{\forall} P_i = P_j \text{ or } \underset{i\in in, j\in out}{\forall} p_i = p_j \tag{14}$$

$$\sum_{i\in in} c_{pi}|Q_i|T_i = \sum_{i\in out} c_{pi}|Q_i|T_i \tag{15}$$

3.2. Coupling method of pipe networks

The gas collection pipe network is used as an example to introduce the coupling method. The node equations method is adopted to describe the pipe network. The pipeline hydraulic equations (Eqs. (9) and (11)) can be transformed into the relationship between pipeline flow and node pressure. Moreover, these equations are taken into the node equations (Eqs. (13) and (14)) to obtain a system of equations between the node pressure and node flow. This system of equations can be solved to determine the node pressure and pipeline flow [17].

The relationship between pipeline and node flow is derived from the principle of flow balance at each node, as follows:

$$\boldsymbol{AQ} = \boldsymbol{q} \tag{16}$$

where $\boldsymbol{Q} = [Q_1, Q_2, \cdots, Q_n]^{\mathrm{T}}$ is the vector of pipeline gas volume flow rate at standard conditions, $\boldsymbol{q} = [q_1, q_2, \cdots, q_n]^{\mathrm{T}}$ is the vector of node gas volume flow rate at standard conditions. The above pipeline pressure drop can also be described as follow:

$$\Delta\boldsymbol{P} = -\boldsymbol{A}^{\mathrm{T}}\boldsymbol{P} \tag{17}$$

where $\Delta\boldsymbol{P} = [\Delta P_1, \Delta P_2, \cdots, \Delta P_n]^{\mathrm{T}}$ is the vector of square difference of pipeline gas pressure, $\boldsymbol{P} = [P_1, P_2, \cdots, P_m]^{\mathrm{T}}$ is the vector of square of node gas pressure. The simulation method for the gas production network is similar to that of the gas collection network, with the difference that the node flow balance is based on the mass flow rate and node pressure is adopted as the calculation parameter.

The coupling parameter for the gas production system is the flow rate of the collection station. The following procedure is adopted to calculate the pressure and flow rate of the collection station for the two types of pipe networks: For the collection pipe network, Flow rate of the collection station (the boundary node of this network) is used to compute its pressure. For the production pipe network, Pressure of the collection station (the boundary node of this network) is used to compute its gas flow rate. Flow rate of the collection station is iteratively adjusted until the collection and production pipe networks are coupled.

4. Pipe network simulation method combining characteristic curve of compressors

4.1. Hydraulic and thermal boundary models of equipment

Centrifugal compressors, reciprocating compressors, and valves are commonly utilized in gas field pipe networks. The parameters of the equipment model can be partially linearized to establish a relationship (Eq. (18)) between the square of inlet pressure, the square of outlet pressure, and the volume flow, also referenced as the general model. Additionally, due to the insensitivity of flow properties to temperature, a point-by-point iteration can be adopted to calculate the thermal model as follows:

$$aP_{in} + bP_{out} + cQ = d \tag{18}$$

where a, b, c, d are the parameters. As shown in Table 2, the model parameters for equipment with simple hydraulic characteristics are given.

In practical production processes, variations in compressor speed can significantly impact the flow of the entire pipe network. The speed of compressor must be introduced into the model to the need for frequent adjustments. We derive a general model for compressors at variable speed and valves.

4.1.1. Hydraulic model of variable speed centrifugal compressors

The available energy head and characteristic equations for centrifugal compressors [36] are as follows:

$$H = \frac{m}{m-1} Z_{in} R_g T_{in}\left[\left(\frac{p_{out}}{p_{in}}\right)^{\frac{m-1}{m}} - 1\right] \tag{19}$$

$$H = a_1\left(\frac{n}{n_0}\right)^2 + b_1 Q\left(\frac{n}{n_0}\right) + c_1 Q^2 \tag{20}$$

where H is the available energy head, R_g is the gas constant, n is the rotational speed, n_0 is the reference rotational speed, m is the gas variability index. Eq. (19) is the theoretical equation, while Eq. (20) is the fitted equation. Generally, the parameters of Eq. (20) are known. By combining Eqs. (19) and (20), a relationship between pressure ratio, rotational speed, and flow rate can be obtained as follows:

$$\left(\frac{p_{out}}{p_{in}}\right)^{\frac{m-1}{m}} = \frac{m-1}{Z_{in}RT_{in}m}\left[a_1\left(\frac{n}{n_0}\right)^2 + b_1 Q\left(\frac{n}{n_0}\right) + c_1 Q^2\right] + 1 \tag{21}$$

The parameters of the equipment model for Eq. (21) need to be further derived. By bringing the square of the pressure into Eq. (21), we can get as follows:

$$\left(\frac{P_{out}}{P_{in}}\right)^{\frac{m-1}{2m}} = \frac{m-1}{Z_{in}RT_{in}m}\left[a_1\left(\frac{n}{n_0}\right)^2 + b_1 Q\left(\frac{n}{n_0}\right) + c_1 Q^2\right] + 1 \tag{22}$$

Further, by transforming Eq. (22), the relationship between P_{in} and P_{out} can be obtained as follows:

$$\left\{\frac{m-1}{Z_{in}RT_{in}m}\left[a_1\left(\frac{n}{n_0}\right)^2 + b_1 Q\left(\frac{n}{n_0}\right) + c_1 Q^2\right] + 1\right\}^{\frac{2m}{m-1}} P_{in} - P_{out} = 0 \tag{23}$$

Thus, a general model of the centrifugal compressor at variable speeds is obtained in the form of the pressure ratio, as follows:

$$\begin{cases} a = \left\{\dfrac{m-1}{Z_{in}RT_{in}m}\left[a_1\left(\dfrac{n}{n_0}\right)^2 + b_1 Q\left(\dfrac{n}{n_0}\right) + c_1 Q^2\right] + 1\right\}^{\frac{2m}{m-1}} \\ b = -1 \\ c = 0 \\ d = 0 \end{cases} \tag{24}$$

Table A1
Well data.

Well	Gas flow rate ($10^4 m^3/d$)	Water flow rate (m^3/d)	Well	Gas flow rate ($10^4 m^3/d$)	Water flow rate (m^3/d)
1	4.0618	0.49	11	5.8611	0.7
2	8.0748	0.7	12	0.6681	0.05
3	7.87	0.7	13	0.5657	0.05
4	6.0171	0.51	14	1.8529	0.19
5	4.9882	0.42	15	1.3361	0.09
6	0.6681	0.05	16	1.2337	0.09
7	4.7299	0.38	17	4.1154	0.54
8	3.8034	0.28	18	5.9879	0.81
9	2.7257	0.23	19	2.5278	0.18
10	1.6968	0.14	20	1.2337	0.1

4.1.2. Hydraulic model of variable speed reciprocating compressors

The performance characteristics of reciprocating compressors are intrinsically linked to their stroke and cylinder dimensions. According to Stosic's book [37], a relationship between speed and exhaust volume can be obtained as follows:

$$Q = \frac{T_{in} p_S Z_{in}}{T_S p_{in}} \lambda_l \lambda_p \lambda_T \left\{ 1 - \alpha \left[\left(\frac{p_{out}}{p_{in}} \right)^{\frac{1}{m}} - 1 \right] \right\} V_h n \tag{25}$$

where p_S and T_S are the standard pressure and temperature, respectively. λ_l,λ_p, λ_T, α, V_h are the equipment parameters detailed in Stosic's book [37]. A general model of the reciprocating compressor at variable speed is also obtained in the form of the pressure ratio, as follows:

$$\begin{cases} a = \left(-\dfrac{Q T_S p_{in}}{V_h n T_{in} p_S Z_{in} \lambda_l \lambda_p \lambda_T \alpha} + \dfrac{1}{\alpha} + 1 \right)^{2m} \\ b = -1 \\ c = 0 \\ d = 0 \end{cases} \tag{26}$$

4.1.3. Thermal model of compressors

The thermal models of centrifugal and reciprocating compressors are identical and are based on the principle of constant entropy [38], as follows:.

$$T_{out} = T_{in} \left(\frac{p_{out}}{p_{in}} \right)^{\frac{m-1}{m}} \tag{27}$$

4.1.4. Hydraulic and thermal models of valve

The valve regulates the inlet and outlet pressures by controlling the flow coefficient. The hydraulic model for the valve is as follows:

$$Q = C_d \sqrt{\frac{2(p_{in} - p_{out})}{\rho_{in}}} \tag{28}$$

Similarly, a general model of the valve is obtained as follows:

$$\begin{cases} a = \left(1 - \dfrac{\rho_{in}}{2 p_{in}^{(n)} C_d^2} Q^2 \right)^2 \\ b = -1 \\ c = 0 \\ d = 0 \end{cases} \tag{29}$$

Table A2
Pipeline data.

Pipeline	Inlet node	Outlet node	Length (km)	Diameter (mm)	Pipeline	Inlet node	Outlet node	Length (km)	Diameter (mm)
1	6	22	1.79	58	11	10	22	3.44	69
2	12	22	2.71	69	12	1	22	2.38	58
3	13	22	4.01	58	13	7	22	0.84	58
4	20	22	7.17	58	14	17	22	5.90	58
5	16	22	5.64	90	15	11	22	2.47	58
6	8	22	2.08	69	16	4	22	1.86	69
7	19	22	6.61	69	17	5	22	5.65	69
8	9	22	4.30	44	18	18	22	5.48	69
9	14	22	6.77	69	19	3	22	2.06	69
10	15	22	4.74	69	20	2	22	1.63	90

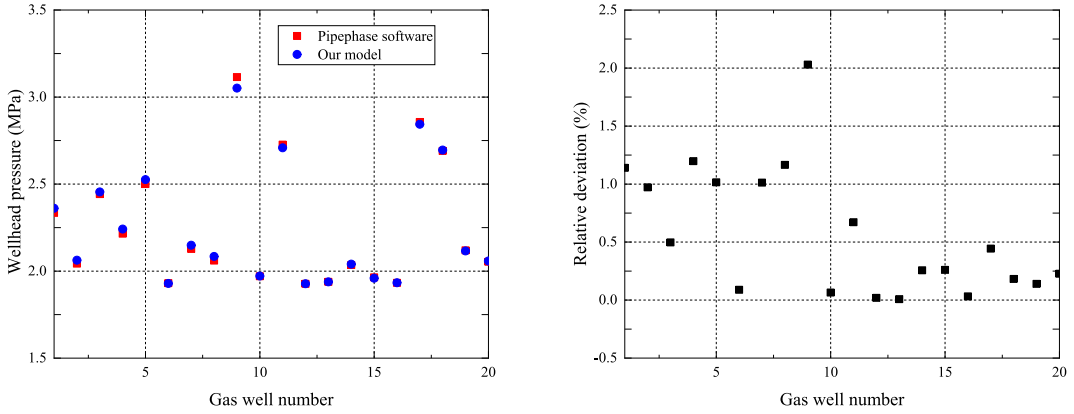

(a) Wellhead pressure. (b) Relative deviation of wellhead pressure.

Fig. 9. Model validation.

Table B1
Node data.

Node	Node type	Pressure (MPa)
1	Collection station	5.09
2	Collection station	5.18
3	Collection station	5.23
4	Collection station	5.09
5	Collection station	5.16
6	Collection station	5.09
7	Collection station	5.16
8	Collection station	5.18
9	Collection station	5.01
10	Collection station	5.06
11	Collection station	5.23
12	Collection station	4.51
13	Connection node	/
14	Connection node	/
15	Connection node	/
16	Connection node	/
17	Purification plant	5.09

Table B2
Pipeline data.

Pipeline	Inletnode	Outletnode	Length (km)	Diameter (m)	Flow rate ($10^5 m^3/d$) (MPa)
1	2	1	8.79	0.257	5.47
2	3	2	8.87	0.205	2.33
3	3	4	10.27	0.257	6.49
4	4	1	9.87	0.205	0.48
5	5	1	13.54	0.257	3.91
6	6	4	8.73	0.257	4.15
7	6	14	9.87	0.3113	10.36
8	7	6	2.78	0.205	4.79
9	8	14	12.18	0.205	3.93
10	9	14	10.42	0.257	2.58
11	10	9	7.26	0.205	2.37
12	11	3	7.97	0.205	0.46
13	12	17	11.08	0.257	2.17
14	1	13	10	0.257	7.15
15	13	17	9.2	0.257	16.07
16	11	13	10	0.307	11.36
17	13	16	9.2	0.307	25.51
18	4	13	15.5	0.4412	23.08
19	14	17	20.5	0.307	16.87

The principle of constant enthalpy [39] is adopted as the thermal model for valves, as follows:

$$T_{out} - T_{in} + (p_{out} - p_{in})\left\{\frac{1}{c_p}\left[\frac{T(\partial p/\partial T)_\rho}{\rho^2(\partial p/\partial \rho)_T} - \frac{1}{\rho}\right]\right\} = 0 \tag{30}$$

In the directed graph, the nodes of the equipment and pipeline are set similarly. Thus, two distinct nodes are utilized to represent the inlet and outlet of the equipment. The inlet node is typically designated as the pressure boundary, while the outlet node as the flow boundary. From the general model of compressors and valves, the parameters are only related to the parameters of the equipment inlet. Consequently, it is imperative to accurately update the inlet parameters during the iterative process. This is also the key reason to set the inlet of the equipment to the pressure boundary.

4.2. Solving methods of pipe network

Two primary methods for solving large-scale pipe network problems are the Newton-Raphson method [21] and the linear approximation method [22]. The natural gas production system includes two types of pipe networks with different calculation parameters, which pose challenges for the computational stability and efficiency. The Newton-Raphson method takes Eq. (9) directly into Eqs. (16) and (17) to form

Table B3
Well data.

Well	Node	Flow rate ($10^4 m^3/d$)	Diameter (mm)	Length (km)
1	1	0.5	69	4.19
2	1	1	58	1.794
3	1	1	69	2.708
4	1	1	58	4.01
5	1	1	58	7.169
6	1	1.5	90	5.635
7	1	2	69	2.082
8	1	2	69	6.61
9	1	3	44	4.3
10	1	3	69	6.768
11	1	3	69	4.74
12	1	4	69	3.44
13	1	4.5	58	2.379
14	1	7	58	0.84
15	1	7	58	5.9
16	1	7.5	58	2.467
17	1	8	69	1.86
18	1	9	69	5.65
19	1	9	69	5.48
20	1	10	69	2.055
21	1	11	90	1.63
22	2	0.2	58	4.433
23	2	0.2	44	3.256
24	2	0.2	44	3.041
25	2	0.3	58	4.184
26	2	0.5	44	1.8
27	2	3	58	2.787
28	2	4.5	69	5.15
29	2	6	69	0.284
30	2	7.5	69	2.991
31	2	9	69	4.5
32	3	0.4	44	4.639
33	3	0.8	58	4.665
34	3	1.2	44	6.925
35	3	1.5	44	2.22
36	3	2.2	58	3.507
37	3	3.5	58	3.4
38	3	3.5	69	7.843
39	3	5	90	5.159
40	3	5	69	4.935
41	3	5	69	4.382
42	3	5	90	5.227
43	3	5.5	69	5.835
44	3	6	58	0.285
45	3	6	58	2.421
46	3	8	90	2.975
47	3	12	69	4.153
48	3	13	90	1.97
49	4	0.2	44	3.35
50	4	0.5	44	4.49
51	4	2	58	4.2
52	4	2.5	90	6.42
53	4	2.5	69	4.577
54	4	3.5	58	5.17
55	4	4.5	44	2.977
56	4	5	58	5.44
57	4	5	58	3.47
58	4	5.5	58	2.187
59	4	5.5	69	7.193
60	4	6	69	3.85
61	4	6	58	1.86
62	4	6	58	4.12
63	4	10	58	2.35
64	4	14	90	3.787
65	4	15	69	3.05
66	4	15	90	3.145
67	4	15	90	4.975
68	4	15	90	6.31
69	4	16	90	0.245
70	5	0.1	58	4.782
71	5	0.2	44	6.16
72	5	0.2	44	7.26
73	5	0.2	44	4.194
74	5	0.2	44	5.998

(continued on next page)

Table B3 (*continued*)

Well	Node	Flow rate ($10^4m^3/d$)	Diameter (mm)	Length (km)
75	5	0.2	44	5.485
76	5	0.2	69	4.352
77	5	0.3	44	3.41
78	5	0.5	44	6.239
79	5	0.5	44	3.158
80	5	0.8	44	0.85
81	5	1	44	5.18
82	5	1.2	58	3.6
83	5	1.5	44	6.721
84	5	1.5	58	1.512
85	5	2	69	7.776
86	5	2.5	58	5.31
87	5	2.5	69	5.371
88	5	2.5	44	0.086
89	5	3.5	58	4.146
90	5	3.5	69	4.98
91	5	7	69	7.437
92	5	7	69	4.5
93	6	0.2	44	6.17
94	6	0.2	58	3.65
95	6	0.2	44	5.87
96	6	0.5	44	2.819
97	6	1	58	2.239
98	6	1	58	2.966
99	6	3	58	0.588
100	6	6	69	6.123
101	6	9	90	2.221
102	6	9	90	1.8
103	6	11	69	5.893
104	6	21	90	3.683
105	7	0.2	44	1.77
106	7	0.2	44	1.97
107	7	0.5	44	3.58
108	7	1	44	2.39
109	7	2.5	58	3.065
110	7	2.5	44	1.563
111	7	3.5	58	6.45
112	7	3.5	58	6.179
113	7	7	44	4.65
114	7	9	69	3.24
115	7	18	69	0.785
116	8	0.2	58	5.302
117	8	0.2	44	3.555
118	8	0.2	44	6.713
119	8	0.2	44	1.51
120	8	0.2	58	3.32
121	8	0.2	44	2.095
122	8	0.2	44	3.007
123	8	0.2	44	4.71
124	8	0.2	44	5.247
125	8	0.5	58	4.081
126	8	0.5	69	5.063
127	8	1	44	1.664
128	8	1	58	4.26
129	8	1	58	0.58
130	8	1.5	58	6.802
131	8	2	69	6.68
132	8	2	69	2.21
133	8	2	44	3.835
134	8	2.5	58	2.71
135	8	3.5	58	4.88
136	8	5.5	69	3.67
137	8	6.5	58	2.88
138	8	8	90	2.49
139	9	0.1	44	2.586
140	9	0.2	44	2.07
141	9	0.3	44	3.39
142	9	0.5	44	3.925
143	9	1	44	3.01
144	10	0.2	58	5.48
145	10	0.5	58	4.14
146	10	1	44	3.387
147	10	1.5	58	1.36
148	10	1.5	58	2.895
149	10	4	69	4.1
150	10	5	90	6.28

Table B3 (*continued*)

Well	Node	Flow rate ($10^4m^3/d$)	Diameter (mm)	Length (km)
151	10	10	90	2.69
152	11	0.2	44	6.68
153	11	0.2	44	6.819
154	11	0.2	44	3.46
155	11	0.2	44	3.53
156	11	0.5	44	3.45
157	11	0.5	44	1.47
158	11	0.5	44	0.803
159	11	0.5	44	1.892
160	11	0.8	58	6.654
161	11	1	90	4.077
162	12	0.2	44	4.96
163	12	0.2	44	3.86
164	12	0.2	44	2.83
165	12	0.5	58	1.6
166	12	1.4	58	4.2
167	12	3	58	0.75
168	12	3.2	58	3.52
169	12	6	69	2.32
170	12	7	58	2.6

a nonlinear system of equations, as follow:

$$-\boldsymbol{A}\left(\boldsymbol{S}^{-1}\cdot\boldsymbol{A}^{\mathrm{T}}\boldsymbol{P}\right)^{\frac{1}{\alpha}}=\boldsymbol{q} \tag{31}$$

The dot represents multiplications or powers of the corresponding elements of the matrix. However, the linear approximation method reduces Eq. (9) to a linear relationship between pipeline pressure drop and flow, as follows:

$$\Delta P=S\left|Q^{\alpha-1}\right|Q \tag{32}$$

where $\left|Q^{\alpha-1}\right|$ is the previous iteration value. By taking Eq. (32) into Eqs. (16) and (17), a linear system of equations can be obtained as follows:

$$-\boldsymbol{A}\left(\boldsymbol{S}^{-1}\cdot\left|\boldsymbol{Q}^{\cdot(1-\alpha)}\right|\right)\cdot\boldsymbol{A}^{\mathrm{T}}\boldsymbol{P}=-\boldsymbol{Y}\boldsymbol{P}=\boldsymbol{q} \tag{33}$$

5. Discussion section

5.1. Model validation

The gas production pipe network exhibits a relatively simple structure, consisting of several wellheads connected to a single collection station. We adopt the field data from a natural gas production system in China to validate our model. As only water and gas flow rate data are available for production pipelines, for the production pipe network, our model is compared to the Pipephase software. The inlet pressure at the gas collection station is 1.92 MPa. The wellhead pressure is calculated based on the wellhead mass flow rate. Relevant parameters are detailed in Table A1 and A2. The comparison results are as follows:

As shown in Fig. 9, our model results are consistent with the Pipephase software results, with a maximum relative deviation of 2.03 %. Due to the limitations of the simulation software in handling both multiphase and single-phase flow pipe networks, the field data from the design stage is used to verify the accuracy of the coupled model, as detailed in Table B1, B2 and B3. Similarly, Pipephase software is used to validate the wellhead pressure. The field data of the collection pipe network is used to validate flow rate of the collection pipelines and outlet pressure of the collection stations. The comparison results are as follows:

As shown in Fig. 10 (c-f), the results of our model are consistent with the field data. The relative deviations of flow rate of collection pipelines and outlet pressure of the collection stations are all within 3 %. This indicates that the model presented in this study possesses a satisfactory level of accuracy.

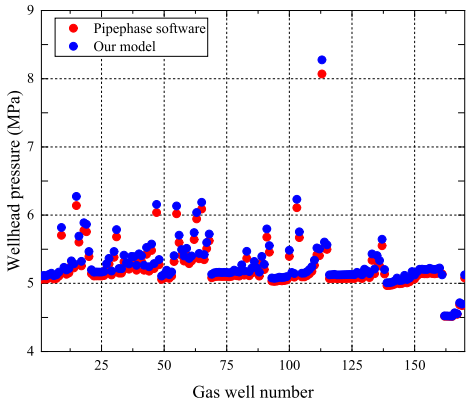

(a) Wellhead pressure.

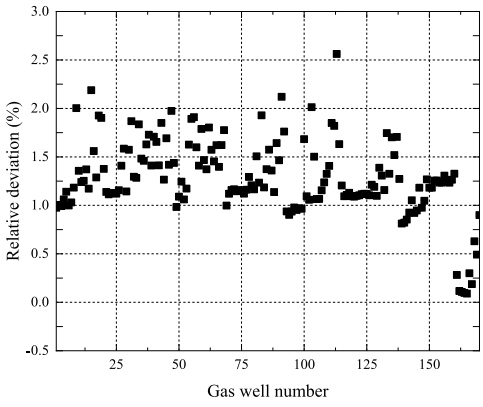

(b) Relative deviation of wellhead pressure.

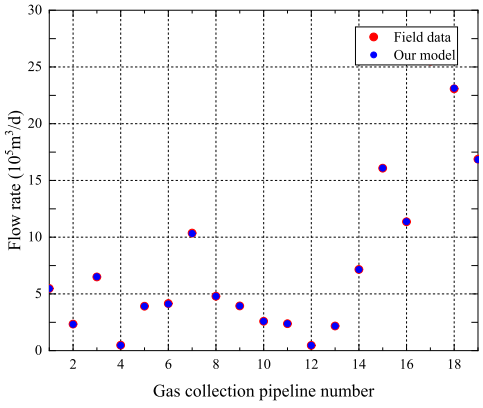

(c) Flow rate of the collection pipelines.

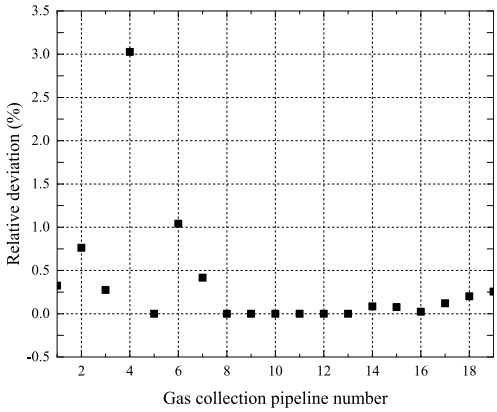

(d) Relative deviation of flow rate of the collection pipelines.

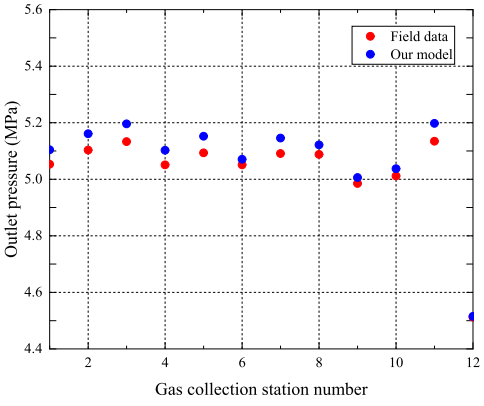

(e) Outlet pressure of the collection stations.

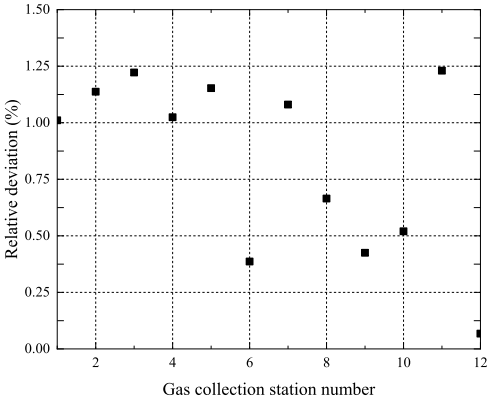

(f) Relative deviation of outlet pressure of the collection stations.

Fig. 10. Model validation.

5.2. *Case of complex and large-scale pipe networks*

A gas field network in China is used as an example [40]. The network comprises 210 nodes and 176 pipelines, including 114 collection stations, 33 booster stations, 25 valves, and 5 purification plants. The environmental temperature can be assumed to be 15.35℃. BWRS model [41] is adopted as the gas physical model. Panhandle A equation [42] is adopted as the friction equation. By using the node numbering method proposed in this paper, only the type of node boundary conditions need to be input, and the node numbering is completed automatically. The time spent is reduced from nearly one day manually to within 1 h.

The pressure ratios for all compressors are set to 1.3. Valves 10, 11, 12, 18, 19, 20, 21, and 24 are closed, while all other valves remain fully open to achieve regional pressurization. The comparison results are as

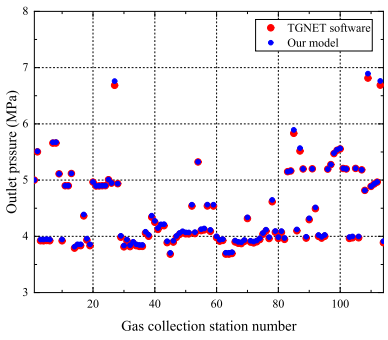

(a) Outlet pressure of collection stations.

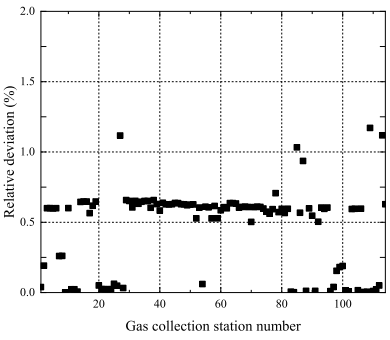

(b) Relative deviation of outlet pressure of the collection stations.

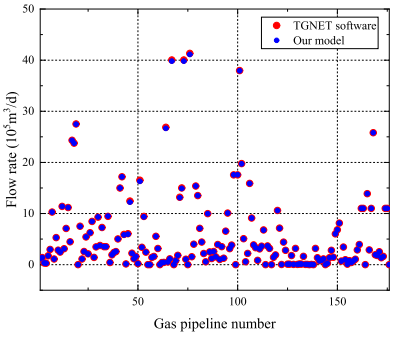

(c) Flow rate of the pipelines.

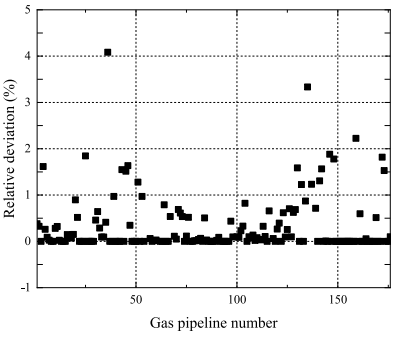

(d) Relative deviation of flow rate of the pipelines.

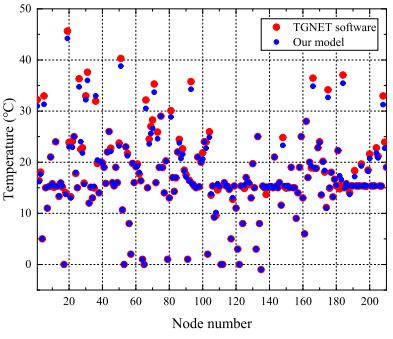

(e) Node temperature.

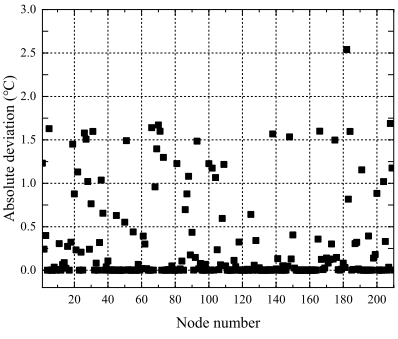

(f) Absolute deviation of node temperature.

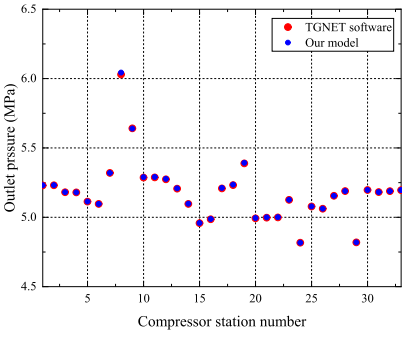

(g) Outlet pressure of compressor stations.

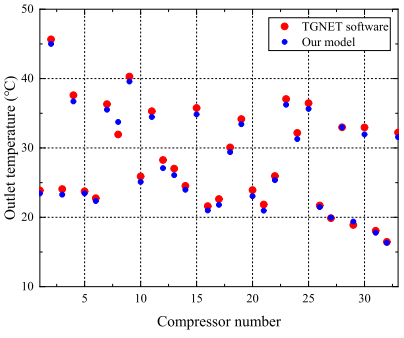

(h) Outlet temperature of compressor stations.

Fig. 11. Comparison results.

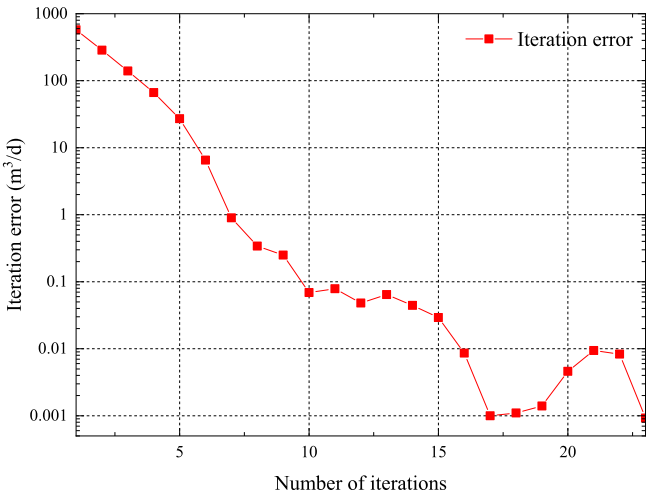

Fig. 12. Variation of iteration error with number of iterations.

follows:

As shown in Fig. 11, our model results are in general agreement with the TGNET software simulation results, with the relative deviation of outlet pressure of the collection stations within 1.2 %, the relative deviation of flow rate of the pipelines within 4 %, and the absolute deviation of the node temperature within 2.5℃. It can be concluded that the proposed models and methods are applicable to large-scale complex pipeline system. As shown in Fig. 12, the iteration error variation for flow rate is stabilized during the iteration process.

Our new model may have some impact on computational stability. We analyze the applicability of the solving methods to the new model. The above large-scale pipe network model is re-simulated by different initial values of node pressure and pipeline pressure drop. The computational stabilities are shown in Tables 3 and 4.

As shown in Table 4, The Newton-Raphson method fails to converge and the linear approximation method succeeds for initial value of pipeline pressure drop of 10^{10}MPa. This suggests that the linear approximation method is more robust than the Newton-Raphson method (implemented in TGNET software). Moreover, the linear approximation method requires fewer iterations than the Newton-Raphson method, as shown in Table 3 and 4. The linear approximation method outperforms the Newton-Raphson method in terms of convergence and computational speed. The order of magnitude of the initial values is based on the typical range of node pressure and pipeline pressure drop in natural gas production system. Therefore, initial values of node pressure and pipeline pressure drop are set as 5 MPa and 10^{-1}MPa, respectively.

5.3. Case of variable speed reciprocating compressors

The reciprocating compressor is used to achieve regional pressurization. A case is set as an example of a wellhead pressure of 4.0 MPa reported in the literature [43]. The structure of the pipe network is shown in Fig. 13. The adaptability of the reciprocating compressors coupled with the pipe network model can be verified.

The speeds of compressors 1 and 2 are adjusted as indicated in Table 5. The inlet pressure of compressors 3 and 4 are set to 3.1 MPa and 2.9 MPa, respectively.

The simulation results of the compressor are as follows:

As shown in Fig. 14, the flow rate of compressors 1 and 2 increases with increased compressor speed. Compressor 2 has a higher speed than compressor 1, resulting in a greater flow rate for compressor 2. According to the production demand, the flow rate of the collection stations is generally fixed. Compressors 1, 2, and 3 can interact within the same ring, leading to an increase in the flow rate of compressors 1 and 2 and a decrease in the flow rate of compressor 3. As the flow rate of compressors 1 and 2 increases, the inlet pressure of the compressors becomes lower. In Fig. 14, we can see that for condition (1) and compressor 1, the inlet pressure is higher than the outlet pressure. The pressure of nodes 1, 2 and 3 is higher than the pressure of node 10 and the flow rate of the pipelines is very low in condition, which results in a low pressure drop along the pipelines. Therefore, the inlet pressure is higher than the outlet pressure. Real compressors do not allow this status, but it is difficult to be detected in previous simulations using TGNET software because it cannot converge under working condition (1). However, our model still converges in the pressure ratio less than 1, so that it can detect the unreal status of inlet and outlet pressures. Therefore, our model is more robust and realistic than the TGNET software. The computations in working conditions (2), 3, and 4 are convergent for both TGNET software and our model, the comparison results are as follows:

As shown in Fig. 15, the relative deviation of outlet pressure of gas collection stations is all within 2.0 %. The relative deviation of flow rate of gas pipelines is within 10 %. The primary cause of this deviation is that some equipment parameters in the TGNET software are unknown and unsettable.

Table 3
Computational stabilities for different initial values of node pressure.

Solving method	Initial value of node pressure (MPa)	Initial value of pipeline pressure drop (MPa)	Convergence property	Number of iterations	Calculation time (s)
Newton-Raphson method	0.01	10^{-13}	Convergence	153	3.16
	10	10^{-13}	Convergence	158	3.20
	100	10^{-13}	Convergence	182	3.77
Linear approximation method	0.01	10^{-13}	Convergence	34	0.33
	10	10^{-13}	Convergence	35	0.37
	100	10^{-13}	Convergence	43	0.40

Table 4
Computational stabilities for different initial values of pipeline pressure drop.

Solving method	Initial value of node pressure (MPa)	Initial value of pipeline pressure drop (MPa)	Convergence property	Number of iterations	Calculation time (s)
Newton-Raphson method	5	10^{10}	Divergence	—	—
	5	10^{-1}	Convergence	164	3.47
	5	10^{-14}	Convergence	141	3.01
Linear approximation method	5	10^{10}	Convergence	109	0.91
	5	10^{-1}	Convergence	37	0.43
	5	10^{-14}	Convergence	30	0.34

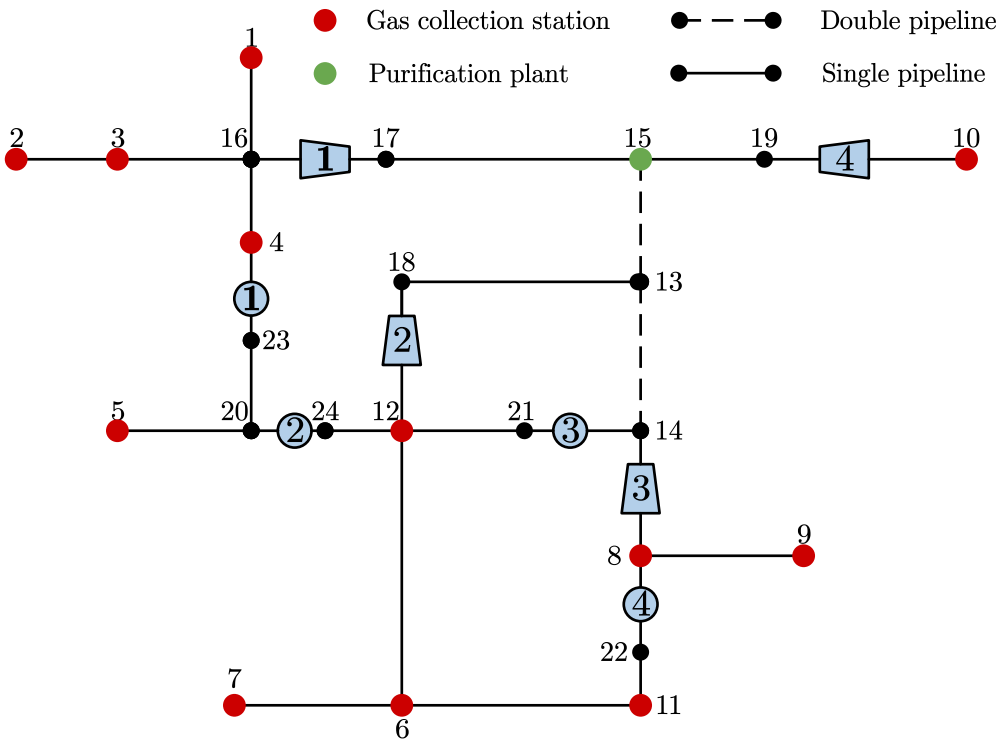

Fig. 13. Structure of the pipe network.

Table 5
Compressor speeds for four working conditions.

Working condition	Speed of compressor 1 (RPM)	Speed of compressor 2 (RPM)
1	500	700
2	1000	1200
3	1400	1600
4	1800	2000

5.4. Case of variable speed centrifugal compressors

A case from the literature [44] is used to verify the adaptability of the centrifugal compressor coupled with the pipe network model. The structure of the pipe network is shown in Fig. 16.

Based on the compressor parameters reported in the literature [44], the characteristic parameters of the compressor are fitted. The energy head-flow characteristic and efficiency-flow characteristic curves at different speeds are shown in Fig. 17.

Compressors 1, 2, 3, and 4 operate at 6019, 6200, 6500, and 6000 RPM, respectively. The results compared with TGNET software are as follows:

As shown in Fig. 18, the simulation results are consistent with the TGNET software results. The relative deviation of pipeline flow is within 6 %, primarily within 1 %. The relative deviations of node pressure and temperature are within 0.8 % and 1.4 %, respectively. Meanwhile, it is noted that the flow rate of pipelines 2 and 3 have a large relative deviation due that the flow rate of pipelines 2 and 3 tend to be close to zero. A small iteration error can result a very large relative deviation.

The operating characteristics of the compressor can be determined, as shown in Fig. 19. The black square in Fig. 18 represents the compressor working point determined by TGNET, and the red dot represents that determined by our model. It can be seen that there is a certain deviation in the energy head and efficiency, which is mainly caused by the following two aspects: (1) There is a certain deviation in the volume of standard condition due to the different gas equations of state used; (2) There is a deviation in the fitted coefficient between our model and TGNET software.

6. Conclusions section

A set of simulation models and numerical methods for simulating complex natural gas production system which involves both multi-phase and single-phase flows in pipe networks and compressor stations is proposed in this paper. The proposed models and methods are validated by comparing with field data, Pipephase software, and TGNET software. The main improvements of this paper are as follows:

An efficient node numbering method can automatically assign node numbers and resolve the boundary condition conflicts between coupling nodes and compressors. A coupled hydraulic-thermal method can simulate the natural gas production system combining single-phase flow and multi-phase flows. Comprehensive compressor models can incorporate the characteristic curves of centrifugal and reciprocating compressors and eliminate the unrealistic assumptions of constant pressure or flow rate boundaries in the simulation of pipe network. The simulation time is only 0.5 s for the pipe network with 210 nodes and 176 pipelines. The results show good agreement with the reference data, with relative deviations within 3 % in both pressure and flow compared to field data and within 10 % compared to software. Our model can also detect and prevent unrealistic situations, such as the inlet pressure of the compressor being higher than its outlet pressure, which are not allowed by the real compressors and are difficult to be detected by the previous simulation software, such as TGNET. The model can achieve convergence even when the pressure ratio is less than 1, which indicates the unreal status of the inlet and outlet pressures.

However, this study also has some limitations that need to be acknowledged and addressed in future research. First, the pipe network model in this study is based on the steady-state assumption, which neglects the transient effects of the flow and temperature variations caused by the frequent adjustments in the operating conditions. Second, the multiphase flow model in this study adopts the existing multi-phase model for pipeline, which has some limitations in calculating the

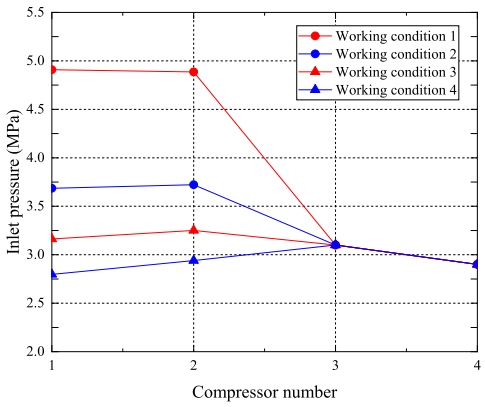

(a) Inlet pressure of the compressors.

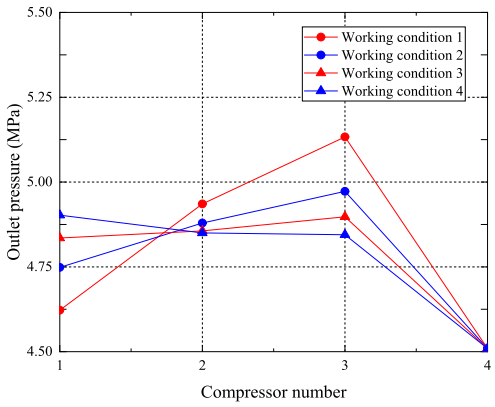

(b) Outlet pressure of the compressors.

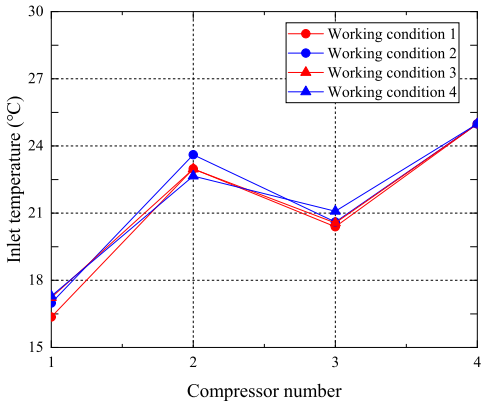

(c) Inlet temperature of the compressors.

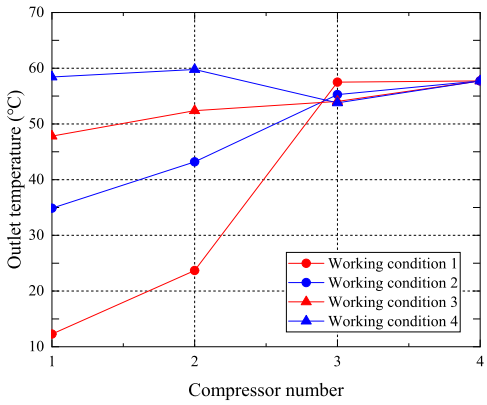

(d) Outlet temperature of the compressors.

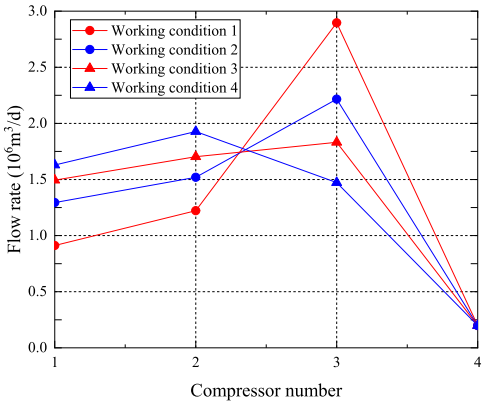

(e) Flow rate of the compressors.

Fig. 14. Simulation results of the compressors.

pressure drop and may introduce some modeling errors.

Therefore, future studies of the natural gas production system should incorporate a transient model for the pipe network and use more advanced and accurate multiphase flow models, to enhance the reliability and robustness for the natural gas production system.

CRediT authorship contribution statement

Wendi Xue: Conceptualization, Formal analysis, Methodology, Software, Writing – original draft, Writing – review & editing. **Yi Wang:** Supervision, Writing – review & editing. **Yuejiu Liang:** Formal analysis, Resources. **Tianfu Wang:** Methodology, Writing – original draft. **Bowen Ren:** Conceptualization, Software, Visualization.

Declaration of competing interest

The authors declare that they have no known competing financial interests or personal relationships that could have appeared to influence the work reported in this paper.

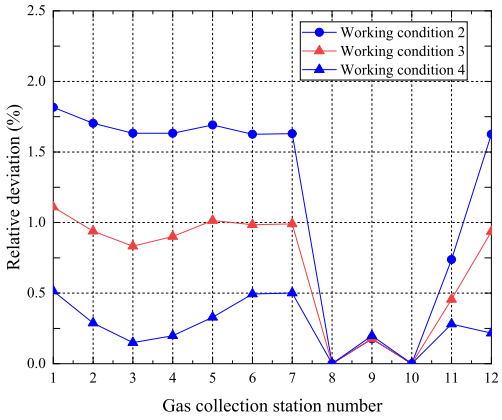

(a) Relative deviation of outlet pressure of gas collection stations.

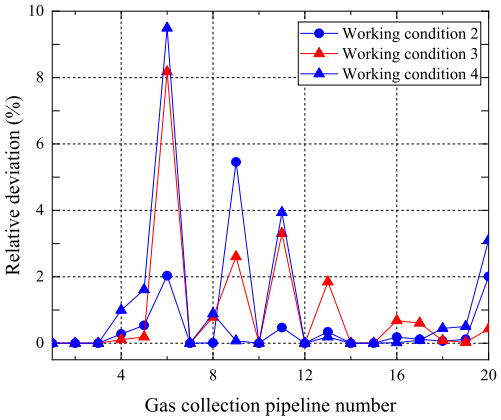

(b) Relative deviation of flow rate of gas collection pipelines.

Fig. 15. Comparison results.

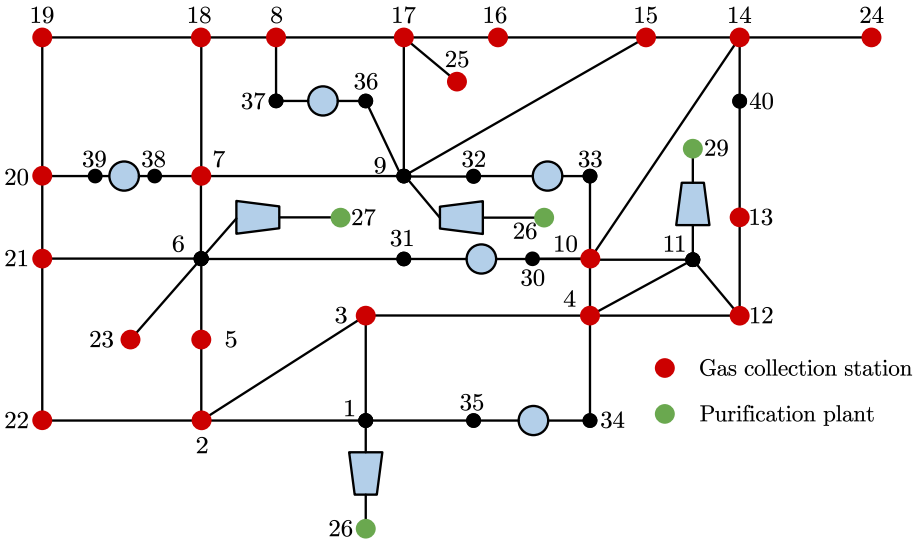

Fig. 16. Structure of the pipe network.

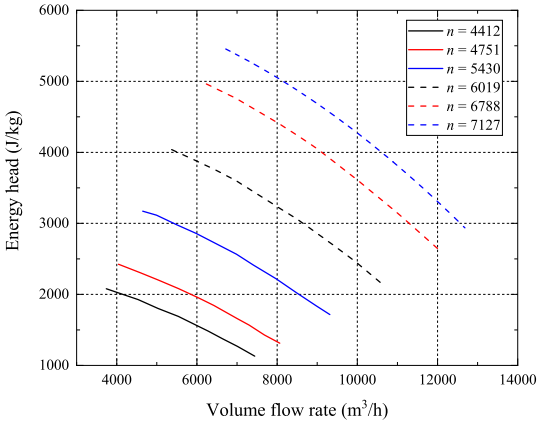

(a) Energy head-flow characteristic curve.

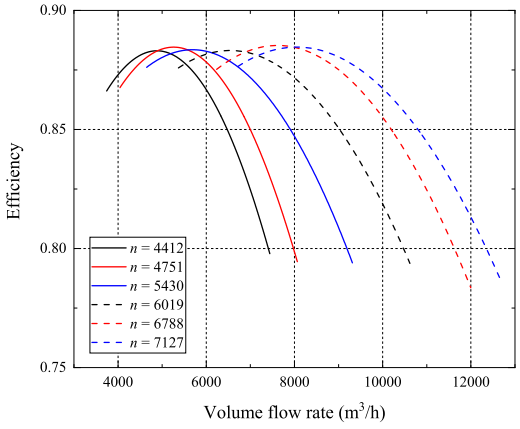

(b) Efficiency-flow characteristic curve.

Fig. 17. Fitted curves.

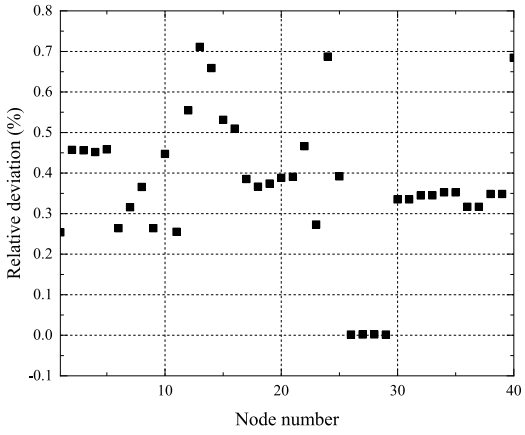

(a) Relative deviation of node pressure.

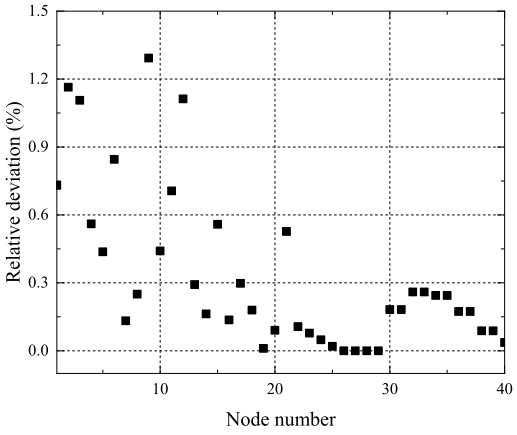

(b) Relative deviation of node temperature.

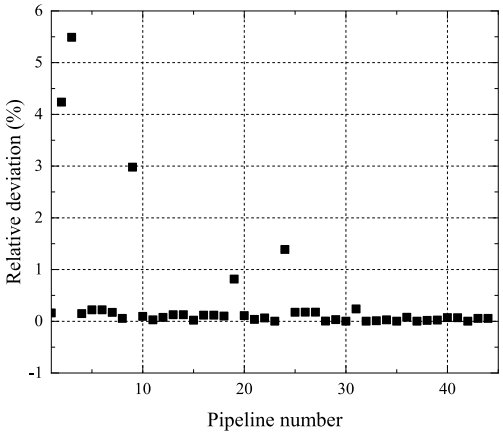

(c) Relative deviation of pipeline flow.

Fig. 18. Comparison of the proposed model and TGNET software.

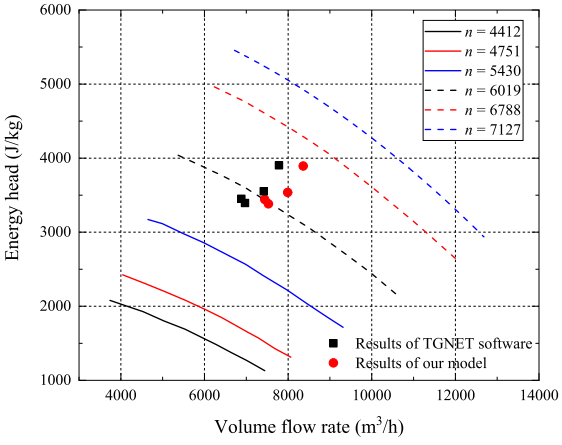

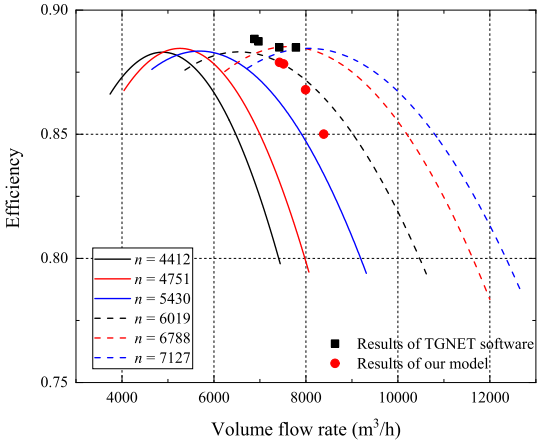

Fig. 19. Working point of compressors.

Data availability

No data was used for the research described in the article.

Acknowledgement

The study is supported by the National Science Foundation of China (No. 51576210).

References

[1] K. Wen, D. Qiao, C. Nie, Y. Lu, F. Wen, J. Zhang, Q. Miao, J. Gong, C. Li, B. Hong, Multi-period supply and demand balance of large-scale and complex natural gas pipeline network: Economy and environment, Energy. 264 (2023), https://doi.org/10.1016/j.energy.2022.126104.

[2] J. Gong, Q. Kang, H. Wu, X. Li, B. Shi, S. Song, Application and Prospects of Multi-phase Pipeline Simulation Technology in Empowering the Intelligent Oil and Gas Fields, J. Pipeline Sci. Eng. (2023) 100127, https://doi.org/10.1016/j.jpse.2023.100127.

[3] Y. Wang, B. Yu, Z. Cao, W. Zou, G. Yu, A comparative study of POD interpolation and POD projection methods for fast and accurate prediction of heat transfer problems, Int. J. Heat Mass Transf. 55 (2012) 4827–4836, https://doi.org/10.1016/j.ijheatmasstransfer.2012.04.053.

[4] Y. Xu, B. Ren, W. Zhao, F. Xu, Y. Wang, Y. Liang, Preliminary Study on Integrated Simulation of Natural Gas Gathering Pipeline Network, Mech. Mach. Sci. 97 (2021) 287–300, https://doi.org/10.1007/978-3-030-64690-5_28.

[5] Y. Li, Y.F. Cheng, C.L. Yan, Z.Y. Wang, L.F. Song, Effects of creep characteristics of natural gas hydrate-bearing sediments on wellbore stability, Pet. Sci. 19 (2022) 220–233, https://doi.org/10.1016/J.PETSCI.2021.10.026.

[6] Y. Zhu, P. Wang, Y. Wang, R. Tong, B. Yu, Z. Qu, Assessment method for gas supply reliability of natural gas pipeline networks considering failure and repair, J. Nat. Gas Sci. Eng. 88 (2021), https://doi.org/10.1016/j.jngse.2021.103817.

[7] Y. Wang, S. Sun, B. Yu, Acceleration of gas flow simulations in dual-continuum porous media based on the mass-conservation pod method, Energies. 10 (2017), https://doi.org/10.3390/en10091380.

[8] Y. Wang, B. Yu, Y. Wang, Acceleration of gas reservoir simulation using proper orthogonal decomposition, Geofluids. 2018 (2018), https://doi.org/10.1155/2018/8482352.

[9] W. Xue, Y. Wang, Z. Chen, H. Liu, An integrated model with stable numerical methods for fractured underground gas storage, J. Clean. Prod. 393 (2023), https://doi.org/10.1016/j.jclepro.2023.136268.

[10] H. Cross, Analysis of flow in networks of conduits or conductors, Eng. Exp. Stn. 34 (1936) 1–29.

[11] D. Brkić, An improvement of Hardy Cross method applied on looped spatial natural gas distribution networks, Appl. Energy. 86 (2009) 1290–1300, https://doi.org/10.1016/j.apenergy.2008.10.005.

[12] M.A. Stoner, Steady-State Analysis of Gas Production, Transmission and Distribution Systems, in (1969), https://doi.org/10.2118/2554-ms.

[13] M.A. Stoner, Sensitivity Analysis Applied To a Steady-State Model of Natural Gas Transportation Systems, Soc Pet Eng J. 12 (02) (1972) 115–125.

[14] G.P. Berard, B.G. Eliason, An Improved Gas Transmission System Simulator, Soc. Pet. Eng. J. 18 (1978) 389–398, https://doi.org/10.2118/6872-PA.

[15] X. Liu, P. Mancarella, Modelling, assessment and Sankey diagrams of integrated electricity-heat-gas networks in multi-vector district energy systems, Appl. Energy. 167 (2016) 336–352, https://doi.org/10.1016/j.apenergy.2015.08.089.

[16] A. Osiadacz, Simulation and analysis of gas networks, (1987) 274. http://www.osti.gov/energycitations/product.biblio.jsp?osti_id=5141539.

[17] A.J. Osiadac, Comparison of numerical methods for steady-state simulation of gas networks, Civ. Eng. Syst. 5 (1988) 25–30, https://doi.org/10.1080/02630258808970499.

[18] A.J. Osiadacz, M. Chaczykowski, Comparison of isothermal and non-isothermal pipeline gas flow models, Chem. Eng. J. 81 (2001) 41–51, https://doi.org/10.1016/S1385-8947(00)00194-7.

[19] J. Szoplik, Improving the natural gas transporting based on the steady state simulation results, Energy. 109 (2016) 105–116, https://doi.org/10.1016/j.energy.2016.04.104.

[20] M. Taherinejad, S.M. Hosseinalipour, R. Madoliat, Dynamic simulation of gas pipeline networks with electrical analogy, J. Brazilian Soc. Mech. Sci. Eng. 39 (2017) 4431–4441, https://doi.org/10.1007/s40430-017-0821-x.

[21] D.W. Martin, G. Peters, The application of Newton's method to network analysis by digital computer, J. Inst. Water Eng. 17 (2) (1963) 115–129.

[22] D.J. Wood, C.O.A. Charles, Hydraulic Network Analysis Using Linear Theory, ASCE J Hydraul Div. 98 (1972) 1157–1170, https://doi.org/10.1061/jyceaj.0003348.

[23] Q. Sun, L.F. Ayala, A linear-rate analog approach for the analysis of natural gas transportation networks, J. Nat. Gas Sci. Eng. 43 (2017) 230–241, https://doi.org/10.1016/j.jngse.2017.03.027.

[24] A. López-Benito, F.J. Elorza Tenreiro, L.C. Gutiérrez-Pérez, Steady-state non-isothermal flow model for natural gas transmission in pipes, Appl. Math. Model. 40 (2016) 10020–10037, https://doi.org/10.1016/j.apm.2016.06.057.

[25] Y. Wang, B. Yu, S. Sun, Fast Prediction Method for Steady-State Heat Convection, Chem. Eng. Technol. 35 (2012) 668–678, https://doi.org/10.1002/ceat.201100428.

[26] A.D. Woldeyohannes, M.A.A. Majid, Simulation model for natural gas transmission pipeline network system, Simul. Model. Pract. Theory. 19 (2011) 196–212, https://doi.org/10.1016/j.simpat.2010.06.006.

[27] A. Bermúdez, J. González-Díaz, F.J. González-Diéguez, Á.M. González-Rueda, M. P. Fernández De Córdoba, Simulation and optimization models of steady-state gas transmission networks, Energy Procedia. 64 (2015) 130–139, https://doi.org/10.1016/j.egypro.2015.01.016.

[28] K.A. Pambour, R. Bolado-Lavin, G.P.J. Dijkema, An integrated transient model for simulating the operation of natural gas transport systems, J. Nat. Gas Sci. Eng. 28 (2016) 672–690, https://doi.org/10.1016/j.jngse.2015.11.036.

[29] D. Zhou, X. Jia, S. Ma, T. Shao, D. Huang, J. Hao, T. Li, Dynamic simulation of natural gas pipeline network based on interpretable machine learning model, Energy. 253 (2022), https://doi.org/10.1016/j.energy.2022.124068.

[30] R.Z. Ríos-Mercado, C. Borraz-Sánchez, Optimization problems in natural gas transportation systems: A state-of-the-art review, Appl. Energy. 147 (2015) 536–555, https://doi.org/10.1016/j.apenergy.2015.03.017.

[31] C. Li, Y. Wang, Z. Chen, G. Liang, Z. Huang, Natural gas pipeline transportation (in Chinese), 2nd ed., Petroleum Industry Press, Beijing, 2008.

[32] Y. Li, G. Yao, The Design and Management of Gas Transmission Pipeline (in Chinese), 2nd ed., China University of Petroleum Press, Shandong, 2009.

[33] Y. Wang, Y. Wang, Z. Cheng, Direct numerical simulation of gas-liquid drag-reducing cavity flow by the VOSET method, Polymers (basel). 11 (2019), https://doi.org/10.3390/polym11040596.

[34] D.H. Beggs, J.P. Brill, A Study of Two-Phase Flow in Inclined Pipes, J. Pet. Technol. 25 (1973) 607–617, https://doi.org/10.2118/4007-PA.

[35] O. Shoham, Mechanistic Modeling of Gas-Liquid Two-Phase Flow in Pipes, Society of Petroleum Engineers, 2006. 10.2118/9781555631079.

[36] K.H. Lüdtke, Process Centrifugal Compressors, Process Centrif. Compressors. (2004), https://doi.org/10.1007/978-3-662-09449-5.

[37] M. Stosic, I. Smith, A. Kovacevic, Screw Compressors - Mathematical Modelling and Performance Calculation, Igarss 2014 (2014) 1–5.

[38] M. Dooner, J. Wang, Compressed-Air Energy Storage, in, Futur. Energy, Elsevier (2020) 279–312, https://doi.org/10.1016/B978-0-08-102886-5.00014-1.

[39] Y. Demirel, V. Gerbaud, Fundamentals of Equilibrium Thermodynamics, in: Nonequilibrium Thermodyn., Elsevier, 2019: pp. 1–85. 10.1016/B978-0-444-64112-0.00001-0.

[40] B. Ren, Study on steady-state hydraulic and thermal simulation of gas field gathering pipeline network (in Chinese), China University of Petroleum (beijing) (2022).

[41] D.G. McFee, K.H. Mueller, J. Lielmezs, Comparison of Benedict-Webb-Rubin, Starling and Lee-Kesler equations of state for use in P-V-T calculations, Thermochim. Acta. 54 (1982) 9–25, https://doi.org/10.1016/0040-6031(82)85060-0.

[42] G.P.S.A. (GPSA), GPSA-Engineering Data Book., 2004.

[43] Y. Jiamao, Research on the Technology of Gathering and Pressure boosting Transportation in Yulin Gas Field Southern District (in Chinese), China University of Petroleum (East China), 2019. https://d.wanfangdata.com.cn/thesis/ChJUaGVzaXNOZXdTMjAyMzAxMTISCUQwMjM0NTk5NhoINGhlNm5nZm0%3D.

[44] P. Wang, Study on the Fast, Accurate and Robust Simulation Method for a Complex Natural Gas Pipeline Network and Its Application (in Chinese), China University of Petroleum (Beijing), 2016.